Catalysis Letters Vol. 104, Nos. 1–2, October 2005 (© 2005)
DOI: 10.1007/s10562-005-7428-z

Catalytic oxidation of ethene on polycrystalline palladium: influence of the oxidation state of the surface

Werner Unterberger[a], Harald Gabasch[a,b], Konrad Hayek[a], and Bernhard Klötzer[a,*]

[a]*Institut für Physikalische Chemie, Leopold-Franzens-Universität, Innrain 52a, A-6020 Innsbruck, Austria*
[b]*Department of Inorganic Chemistry, Fritz-Haber-Institut der Max-Planck-Gesellschaft, Faradayweg 4-6, D-14195 Berlin, Germany*

Received 10 May 2005; accepted 6 July 2005

The partial and total oxidation of ethene was studied on clean and oxidized polycrystalline Pd in a UHV high-pressure cell. The model catalyst was prepared under UHV conditions and characterized by thermal desorption and Auger and Raman spectroscopy. Starting from either a Pd or PdO surface, reaction to CO_2 is the predominant pathway, and acetic acid is the main byproduct between 453 and 523 K. The route to partially oxidized products, in particular acetic acid, is more favoured on the PdO surface, while on Pd metal acetic acid is formed at lower temperatures than on PdO. On stoichiometric PdO activation for both partial and total oxidation occurs during an induction period, until under working conditions Pd metal, PdO, 'PdC_x' and isolated defects are coexistent on the surface. The presence of an extended metal surface favours the follow-up oxidation of byproducts, while the presence of PdO stabilizes acetic acid far beyond 473 K.

KEY WORDS: ultrahigh vacuum; high-pressure cell; palladium; palladium oxide; ethene; acetic acid selective oxidation; model catalyst; phase transformation.

1. Introduction

The oxidation of small hydrocarbons to partially oxidized compounds is governed by the need to suppress total oxidation and to promote selective formation of one particular product. Pd based heterogeneous catalysts such as Pd–Al_2O_3 are known for their superb performance in total oxidation at high temperatures, e.g. of methane or natural gas, and Pd is a major active component in combustion applications like catalytic burners for gas turbines and exhaust control. In the research of catalytic combustion one of the most prominent questions concerns the catalytically active species. Depending on reaction temperature and methaneoxygen feed, either Pd or PdO appears to be the predominant active phase. Recent work has shown that the periodic formation and decay of PdO and Pd metal phases, connected by a variable phase boundary, may explain both the oscillatory reaction kinetics and the particularly active state of the catalyst [1].

On the other hand, the addition of small amounts of Pd to multi-component, mainly molybdenum and vanadium oxide based, catalysts is known to greatly improve their activity and selectivity for partial oxidation to aldehydes and carboxylic acids. Most prominent examples are the oxidation of ethane [2–4] or ethene [5,6] to acetic acid, and of methane to formic acid [7]. Acetic acid formation from ethane is known as a process of great prospective economical interest, and its production from ethene on Pd-promoted heteropolymolybdate is already commercially utilized [6]. Strongly acidic supports appear to favour the selective formation of carboxylic acids.

In all these examples the addition of minute amounts of Pd results in a major increase of the desired selectivities. A common feature of the catalysts for selective ethane oxidation is that they are very active to dehydrogenate ethane to ethene *without* addition of Pd [2]. This suggests a bifunctional catalyst operation: the mixed molybdenum–vanadium oxides catalyze the dehydrogenation to ethene which is then selectively oxidized at Pd-assisted active sites. Although the beneficial role of Pd is an empirical fact, only poor knowledge exists about the nature of its action and its chemical binding and oxidation state under reaction conditions. It is not clear whether the observed catalytic behaviour is an intrinsic property of Pd or a result of cooperative action with the other catalyst components. Early model catalyst studies by Kemball *et al.* [8] have addressed the role of Pd metal in ethene oxidation on evaporated Pd metal films at rather low temperatures, focussing on intermediates, reaction orders and mechanism. They showed that Pd metal catalyzes the total oxidation to CO_2 already around 410 K and that also the metallic state of Pd is capable to produce partially oxidized species, although with less than 1% yield. From present knowledge, these low selectivities are in part explained by a high oxygen-to-ethene ratio, but mainly by the fact that a metallic sample was used, catalyzing at

---

* To whom correspondence should be addressed.
E-mail: bernhard.kloetzer@uibk.ac.at

1011-372X/05/1000–0001/0 © 2005 Springer Science+Business Media, Inc.

a high rate the irreversible dissociation of ethene to carbon and hydrogen and thus leading exclusively to total oxidation.

Several actions are likely to enhance the partial oxidation selectivity of clean Pd from an empirical viewpoint: increasing the ethene to oxygen ratio, co-feeding of steam, reducing the oxidation potential e.g. by hydrogen addition, increasing the total pressure and thereby favouring mass action towards more complex products, and – last but not least – changing the chemical (oxidation) state of the palladium model catalyst. Recent studies of vinyl acetate synthesis on Pd/SiO_2 catalysts have revealed the importance of (sub)surface carbon modification of the Pd surface for improved selectivity [9].

The present work aims at an improved understanding of the oxidation states of Pd catalysts that favour partial versus total oxidation of ethene. Experimentally, such studies must involve the control of the initial state, mainly determined by the chosen preparation procedure, as well as the active state during reaction, which can only be monitored *in-situ*, e.g. by XPS [10]. This study focuses on the effect of the initial catalyst state, prepared and characterized *ex-situ* under UHV conditions. Selectivity studies upon starting from PdO, Pd metal and carbon-modified Pd surfaces were performed in a UHV-compatible high pressure reaction cell, and the final state of the catalyst was also characterized under UHV conditions.

2. Experimental

2.1. Apparatus

Preparation and characterization of the model catalysts were performed under ultrahigh vacuum conditions in an experimental setup described before [11]. It consists of a conventional UHV chamber with a long travel *z*-manipulator and a small-volume Pyrex glass reactor (52 ml) attached to the outside of the chamber and accessible via a sample transfer port. The UHV chamber is equipped with an electron beam heater, an ion sputter gun, a mass spectrometer and an Auger spectrometer. Gases are introduced into the chamber and into the reactor via gas dosing manifolds. Sample transfer is achieved by means of a magnetically coupled transfer rod with a Pyrex glass sample car acting also as sample holder in the reaction cell, with this all-glass setup no wires or thermocouples are connected to the sample during catalytic measurement and therefore background activity is negligible. The main chamber is pumped by a turbomolecular pump, an ion getter pump and a titanium sublimation pump to a base pressure in the low 10^{-10} mbar range. The reaction products were detected either discontinuously by combined gas chromatography/mass spectroscopy (GC-MS, Hewlett Packard G 1800A), or continuously by a direct connection between the reactor and the massselective detector of the latter (see below). High purity gases (C_2H_4, O_2, CO_2, Ar) were used as supplied from Messer-Griesheim.

2.2. Catalyst preparation and reaction conditions

A polycrystalline palladium foil (Goodfellow, purity 99.9%, 0.125 mm thick, size 3 cm^2) was cleaned on both sides by successive cycles of Ar ion bombardment (500 eV, 0.8 μA sample current), oxidation (2.0×10^{-7} mbar O_2, $\leq$1000 K), and annealing in hydrogen (2.0×10^{-7} mbar H_2, $\leq$700 K) and in vacuum (1000 K) until no impurities were detected by AES.

Oxide overlayers were prepared by treating the clean Pd foil at 673 K in 250 mbar O_2 and 750 mbar He in the glass reactor for 2 h. This procedure results in a PdO layer of about 10 nm thickness and was chosen after a detailed investigation of oxide growth with Raman spectroscopy and thermal desorption as described in the result section.

Ethene oxidation was investigated in the temperature range between 373 and 523 K at ethene pressures varying from 1 to 12 mbar and an oxygen pressure of 250 mbar while the reactor was again filled up with He to a total pressure of 1 mbar. In addition, 1 mbar of Ar was added and used as internal standard for calibration of the mass spectrometer during analysis of the reaction mixture.

2.3. Methods of characterization

Raman spectroscopy is a very useful method to analyze the growth of PdO layers since a few Angstrom thick layers are already detectable [12]. Raman spectra were recorded *ex-situ* on a Labram-1B spectrometer equipped with a microscope (Dilor), through an ULWD-50 objective (Olympus), by averaging four sets of spectra. A 20 mW He–Ne Laser with 632.8 nm wavelength was used. Its 1800 L/mm grating provides a resolution of 1.1 cm^{-1} at 150 cm^{-1}, increasing to 0.6 cm^{-1} at 3600 cm^{-1}. The abscissa was calibrated with a silicon standard, and the sharp Raman shifts are accurate to ± 2 cm^{-1}.

Auger measurements were performed *in-situ* with a DESA 100 spectrometer (Staib Instruments). The spectra were acquired at a 3 keV primary energy in the pulse-counting mode and normalized with respect to the background level at the high-energy side of the peaks. Peak shape analysis was performed in the undifferentiated N(E) versus E mode.

2.4. Kinetic measurements

Prior to a reaction, the Pd foil was cleaned until no impurities were detected by AES. Thereafter it was transferred into the preheated high-pressure cell, the preformed reaction mixture was introduced, the capillary leak to the mass spectrometer was opened and conversion and product formation were continuously monitored (see below). At the beginning and end of each reaction, the reaction mixture was also analyzed by static gas chromatography using a sample loop.

The continuous product analysis was achieved by a small gas flow (0.1–0.2 ml/min) through a fused silica capillary, leading from the reactor directly into the mass selective detector of the GC-MS system. As the detector sensitivity turned out to be constantly and significantly lowered by the presence of oxygen in the sample gas, a continuous calibration of the (relative) mass signal intensities was necessary. It was achieved by the above-mentioned internal standard (1 mbar Argon in the reaction mixture). In addition, calibration with external standards of ethene, CO_2 and acetic acid was performed before and after each reaction. As a standard for acetic acid (mass signal 60) we used the saturated vapour phase, thereby accounting for temperature and pressure dependence of the monomer/dimer equilibrium in the gas phase [13].

The conversion of ethene, $X_{C_2H_4} = (p_{C_2H_4,\mathrm{initlal}} - p_{C_2H_4,\mathrm{end}}) / p_{C_2H_4,\mathrm{initial}}$, was determined from the value of the $C_2H_3^+$ signal (mass 27) before reaction and after a given reaction time, usually 30 min. The formation rates of CO_2 and acetic acid were determined with help of the mentioned external standards before and after reaction, while the continuous lowering of all detector signals during reaction was followed by the internal Ar standard. From the corrected mass signals the absolute amounts of CO_2 and acetic acid were calculated. The time-averaged selectivities were usually determined after 30 min reaction time:

$$S_{\mathrm{HOAc}} = p_{\mathrm{HOAc}} / (p_{C_2H_4,\mathrm{initial}} - p_{C_2H_4,\mathrm{end}}),$$

$$S_{CO_2} = p_{CO_2} / (p_{C_2H_4,\mathrm{initial}} - p_{C_2H_4,\mathrm{end}}).$$

From the plots (product pressures vs. time) the time-dependent reaction rates were obtained by differentiation. The reaction rates were converted into turnover frequencies (TOF). The total number of surface sites N_s was determined by assuming the Pd surface (area 6 cm^2) being composed of equally distributed (111) and (100) facets. With this assumption, $N_s = 8.6 \times 10^{15}$ Pd atoms.

3. Results and discussion

3.1. Ethene oxidation on Pd metal

3.1.1. Activity and selectivity trends due to temperature variation

The reaction temperature is most critical because high temperatures favour both dissociation of ethene towards carbon and further oxidation of partially oxidized products to CO_2. At low temperatures (up to 423 K) acetaldehyde and ethene oxide are formed, but on Pd metal the selectivity to ethene oxide is very low (around 0.05%). Acetaldehyde and ethene oxide appear at a constant (temperature-invariant) ratio of about 1:100, indicating the same activation energy of formation. In principle, acetaldehyde may be formed by two different routes: either together with ethene oxide via a single common precursor, or in sequential steps with ethene oxide as a (gas phase) intermediate. In order to discriminate between the two possible mechanisms we measured the oxidation of ethene oxide at different temperatures and at the same oxygen partial pressure. It turned out that ethene oxide is easily oxidized to CO_2 at 403 K (turnover rate about $2 \times 10^{-3}\ s^{-1}$) and above, but not converted to acetaldehyde below 573 K; hence the parallel formation mechanism can be substantiated, according to the oxametallacycle model [14]. The finding that the ratio of ethene oxide to acetaldehyde does not change with temperature (at least in the observed temperature range) can be understood if the formation of the oxametallacycle intermediate is rate-determining and the products are formed according to the statistical distribution of the respective transient states.

Oxidation of acetaldehyde to acetic acid becomes fast at 403 K (TOF about $3.9 \times 10^{-3}\ s^{-1}$).

Figure 1 shows formation rates of acetic acid and CO_2, obtained by differentiation of product versus, time curves, in the temperature range between 423 and 523 K. The TOF for acetic acid reaches a maximum at 473 K and declines with further increasing temperature.

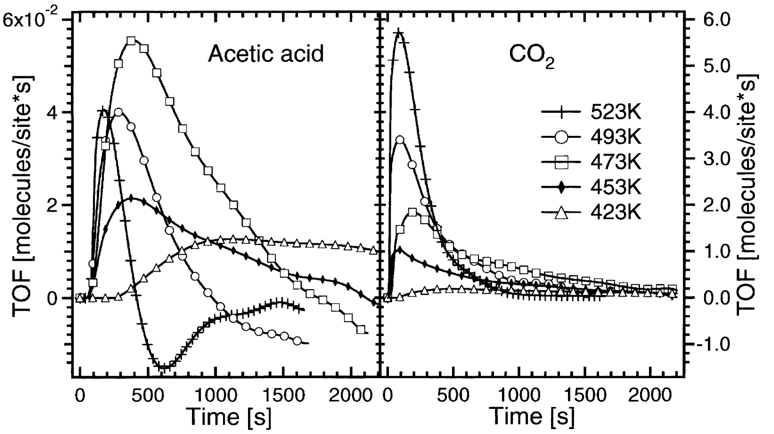

Figure 1. Formation rates of acetic acid (left) and carbon dioxide (right) on pure Pd metal versus reaction time at reaction temperatures between 423 and 523 K.

This can be understood by considering that on palladium metal the oxidation of acetic acid to CO_2 becomes fast at about 473 K. Although the production rate of acetic acid still increases at higher T, its further oxidation leads to the observed effective rate decrease. Consequently, negative formation rates were observed in the course of reactions at higher temperature (e.g. after about 1800 s at 473 K, and earlier and more pronounced at 493 and 523 K; figure 1), indicating that after a certain time more acetic acid is consumed than produced.

With increasing reaction temperature the CO_2 production rises continuously as both direct oxidation and oxidation of intermediate products run at a higher rate. Between 423 and 523 K the increase of CO_2 production is 30-fold and that of acetic acid formation is about 3-fold. Between 473 and 573 K the selectivity to acetic acid decreases from 9.8 to 0.1%, while the total conversion after 30 min rises from 30 to 99% (cf. also figure 5). On the other hand, between 453 and 473 K both acetic acid formation and conversion increase, so that the selectivity remains approximately constant in this narrow temperature range.

These experiments confirm the effectiveness of Pd metal as a catalyst for total oxidation above about 473 K, due to its ability to dissociate ethene, leading to carbon and CO_2, as well as to further oxidize partially oxidized products. The time delay in the formation of acetic acid with respect to CO_2 (figure 1) is most probably caused by its delayed desorption from the catalyst surface. On the other hand, the results summarized in figure 1 show that continuous product analysis under static batch conditions can be used to determine selectivities as a function of 'contact time', hence providing a convenient basis for optimizing contact times in industrial catalytic reactors.

3.1.2. Activity and selectivity trends due to ethene pressure variation

Considering the two reactions

$$C_2H_4 + O_2 \rightarrow CH_3COOH \quad (1)$$

and

$$C_2H_4 + 3O_2 \rightarrow 2CO_2 + 2H_2O, \quad (2)$$

we are likely to assume that an increasing ethene pressure must favour reaction (1). We studied the effect of ethene pressure between 2 and 12 mbar at a constant oxygen pressure of 250 mbar, with helium added to 1 bar total pressure. Figure 2 shows the turnover rates to acetic acid and CO_2 as a function of time at 473 K and varying $p_{C_2H_4}$. Increasing the pressure from 2 to 6 mbar leads to a 4-fold increase of the maximum rate of CO_2 formation, while a pressure rise beyond 6 mbar induces rather small further changes (at $p_{C_2H_4}$ = 12 mbar the rate increase is about 5 fold with respect to the 2 mbar rate). Acetic acid formation, however, is much more affected by changing ethene pressure. Raising$p_{C_2H_4}$ from 2 mbar to 6 and 12 mbar induces a 40- and a 130-fold rate increase, respectively, and a change of acetic acid selectivity from 0.5% (at 2 mbar) to 12.5% (at 12 mbar), as shown in table 1.

Table 1
Total conversion and selectivity to acetic acid after 30 min reaction on Pd metal at 473 K at variable ethene pressure (oxygen pressure 250 mbar, He added up to 1 bar total pressure)

Ethene pressure (mbar)	Conversion after 30 min (%)	Selectivity after 30 min (%)
2	99	0.5
6	85	4.9
12	75	12.5

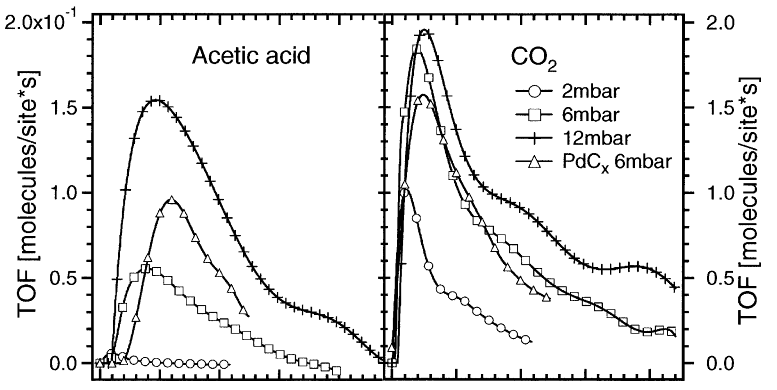

Figure 2. Turnover rates to acetic acid (left) and carbon dioxide (right) on Pd metal as a function of time at varying ethene pressure (2–12 mbar). The effect of a pre-exposure of the surface to 6.0 mbar ethene at 493 K ('PdC_x' surface) is also shown. Reaction conditions: $P_{O_2} = 250$ mbar, $P_{He} = 738$–748 mbar, reaction temperature 473 K.

The above experiments show that a large oxygen excess deactivates the Pd metal surface by blocking the surface, either by oxidic species and/or by chemisorbed oxygen. On the other hand, in a hydrocarbon-rich environment the catalyst is more active and also more selective to acetic acid. We may assume that under these conditions the reduced catalyst surface is in a carbon- (and hydrogen-) modified metallic state. In order to prove this assumption we increased the carbon content of the surface and near-surface bulk regions by exposing the Pd surface to 6.0 mbar ethene at 493 K prior to reaction. At this temperature ethene decomposes and leaves a carbon-modified surface, but C atoms also migrate into surface near regions of the Pd bulk [15,16,9]. The reaction of 6 mbar ethene with 250 mbar oxygen was now repeated, starting from this 'PdC_x' surface as an initial state. As also seen in figure 2, this surface produces less CO_2 and is significantly more selective towards acetic acid than the pure metal.

3.1.3. *Post-reaction analysis*

After every reaction the surface was analyzed with AES under UHV conditions. Only small amounts of chemisorbed oxygen were detected. Although an accurate determination of carbon is hindered by the overlap of the carbon AES signal with the main Pd signal, significant amounts of carbon formed during reaction on the originally clean metal can be excluded because they would induce a characteristic shape change of the Pd signal that was not observed. On the C_2H_4-preexposed surface carbon was identified by subtracting the spectrum of the clean foil from that obtained from the C-modified sample, Recently, carbon deposits on the surface formed under comparable conditions were effectively detected with help of *in-situ* high-pressure XPS [10].

3.2. *Ethene oxidation on a PdO-covered Pd foil*

3.2.1. *Preparation and characterization prior to reaction*

Prior to the catalytic measurements, the growth of PdO overlayers was followed upon exposure of the Pd foil to oxygen at 250 mbar pressure (with He added to 1 bar pressure) at varying T, using Raman spectroscopy, Auger spectroscopy and thermal desorption. Figure 3 shows selected Raman spectra obtained after oxidation for 2 h at different temperatures. With increasing oxidation temperature the main Raman signal at 651 cm^{-1} (B_{1g}-mode) grows while its full width at half maximum decreases, indicating increasingly thicker but better ordered PdO layers (figure 3 right). Also the fine structure of the spectra becomes more pronounced with increasing temperature of exposure. Using isotopic labelling, McBride *et al.* [17] have shown that an exchange of $^{16}O_2$ by $^{18}O_2$ causes the Raman signals *above* the main transition (651 cm^{-1}) to shift towards lower wavenumbers while the signals *below* 651 cm^{-1} remain at the same Raman shift. This is explained by the fact that the high-frequency phonons involve the motion of oxygen atoms in the lattice while the low-frequency phonons arise from the collective motion of Pd. After oxidation at 673 K the fine structure below 651 cm^{-1} is pronounced, but above 651 cm^{-1} it is less developed, which means that the PdO layer is compact enough to ensure concerted Pd motion in the PdO lattice, but contains a high number of oxygen defects, accounting for the poor fine structure on the high frequency side. In contrast, oxidation at 573 K was insufficient to produce PdO layers of adequate thickness and ordering and the spectrum does not exhibit significant fine structure on either side (figure 3).

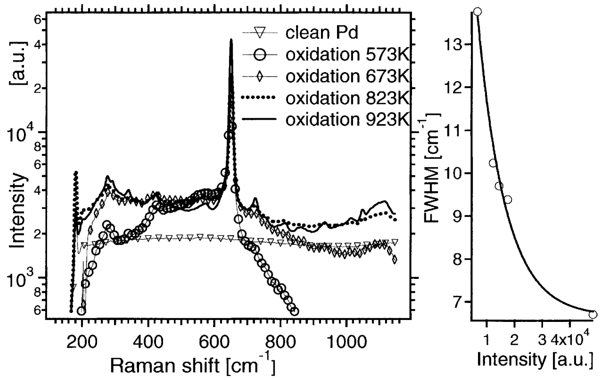

Figure 3. Left: Raman spectra of PdO overlayers prepared at increasing temperature. Right: FWHM versus intensity of the B_{1g}-mode after oxidation at increasing temperature.

Thermal desorption was used to quantify the oxygen content of the NO overlayers. After preparation at varying temperature and oxygen pressure the Pd foil was heated under UHV conditions and the amount of evolved oxygen was determined in the mass spectrometer. It turned out that a treatment in 250 mbar oxygen at 673 K for 2 h results in a layer thickness of about 10 nm, corresponding to about 30 average ML PdO. Auger spectra were also taken before and after thermal desorption. In the oxidized state their characteristic features are a large oxygen signal (KLL transition) and a symmetric shape of the main Pd signal at 330 eV ($M_{45}VV$ transition) (see also Section 3.2.3 and figure 6).

3.2.2. *Activity and selectivity trends*

In figure 4, the turnover rates to acetic acid and CO_2 on clean and oxidized Pd are compared at a (relatively high) reaction temperature of 493 K. The oxidized surface was prepared by exposure to 250 mbar oxygen + 750 mbar He at 673 K for 2 h, On Pd metal the maximum rate of CO_2 formation is almost twice as high as on PdO, but the selectivity to acetic acid is only 1.6% compared to 4.3% on PdO (conversion 95% on Pd, 80% on PdO).

The insert in figure 4 (right) shows that on PdO the onset of CO_2 production is delayed by about 50 s

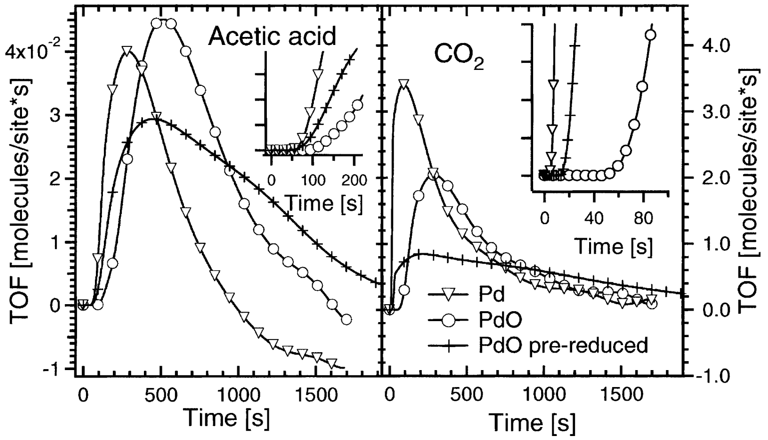

Figure 4. Formation rates of acetic acid and carbon dioxide versus reaction time at 493 K on the metallic and the pre-oxidized Pd surface and on the PdO surface reduced by CO at 473 K.

compared to the metallic surface, This leads to conclude that stoichiometric PdO is not reactive and changes towards a reduced, active state before ethene oxidation sets in. In order to prove this hypothesis the catalyst surface was reduced by exposure to 1 mbar CO for 5 min at 473 K. Indeed, this treatment results in a backshift of the onset of CO_2 formation and to a higher initial activity compared to the fully oxidized surface, but unexpectedly also leads to a change of the general activity-versus-time behaviour of the catalyst (figure 4). Compared to the untreated oxide and the metal surface, the CO-reduced catalyst is significantly more selective to acetic acid. The formation rates of carbon dioxide and acetic acid decrease more slowly and almost steadily with time and negative effective rates towards acetic acid are not observed, in contrast to Pd metal, and – to a smaller extent – also to CO-untreated PdO. While the reduced delay of CO_2 production is most likely related to the CO-induced. pre-formation of oxygen vacancies and/or metallic centres (see AES results, section 3.2.3), the general selectivity trend towards more acetic acid and the altered time-evolution of products are not easily understood. It may be that the pre-reduction by CO and the reaction-induced reduction in ethene/O_2 result in a different size and local distribution of metallic centres among the PdO grains. Tentatively, we may assume that in case of CO pretreatment the dispersion of Pd metal entities/oxygen vacancies is higher, and that they are stabilized by the surrounding PdO environment under reaction conditions. PdO evidently stabilizes acetic acid (see below), while extended metallic Pd surface area favours total oxidation. Hence, highly dispersed metallic centres could well be in favour of selective rather than total oxidation. Apparently, the same conclusion is already implied in the different catalytic behaviour of Pd metal and untreated PdO.

Figure 5 summarizes the total conversion of ethene and the average selectivity to acetic acid, measured after 30 min reaction time, at reaction temperatures between 423 and 523 K on the metallic and oxidized surface. At low reaction temperatures the conversion is low on the oxidized surface, most likely because the initial reductive activation of the PdO surface is suppressed. At 423 K the main product is CO_2, but 5% of acetaldehyde are also formed. With increasing temperature the turnover increases and acetaldehyde is immediately converted to acetic acid. On the metallic Pd surface the selectivity to acetic acid is highest at low temperatures, then decreases and passes a plateau between about 453 and 473 K before declining again. Recent results by Bowker *et al.* [15,16] and Han *et al.* [9] indicate the formation of a carbon-modified surface in this particular temperature range, exhibiting special catalytic properties. This is again confirmed by recent *in-situ* XPS measurements on a Pd(111) single crystal plane [10].

In contrast, on PdO the selectivity to acetic acid is low at low temperature but reaches its maximum (in this

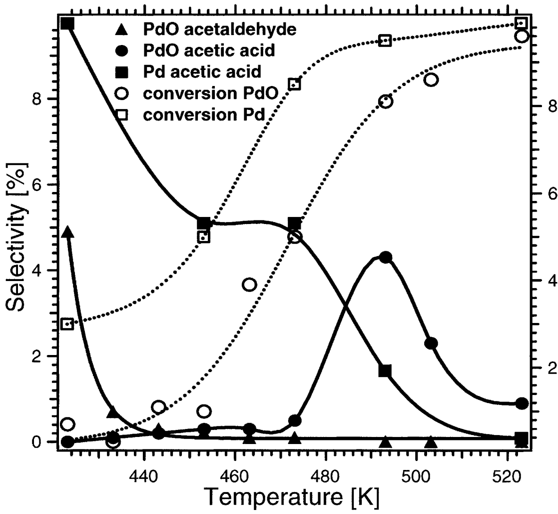

Figure 5. Conversion and (average) selectivity on cleaned and pre-oxidized Pd after 30 min reaction versus reaction temperature. Reaction conditions: 6 mbar ethene, 250 mbar oxygen, 740 mbar He.

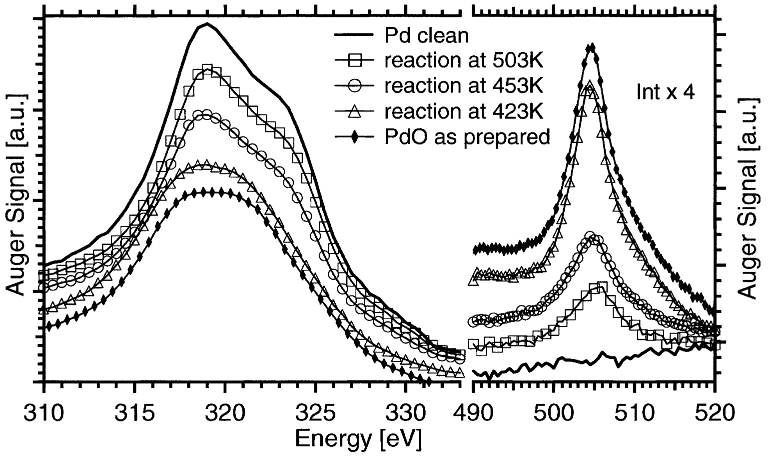

Figure 6. Auger spectra (N(E) versus E) showing the Pd $M_{4,5}VV$ and the O KLL transition from the clean metal surface and from the PdO layer as-grown and after 30 min reaction at 423, 453 and 503 K.

case 4.5%) at 493 K, which is 20 degrees higher than the plateau of acetic acid formation on Pd metal. Presumably, the product acetic acid is stabilized by the Pd^{2+} ions on the PdO surface, forming e.g. Pd-acetates as are known from the literature [18].

3.2.3. Post-reaction analysis

After each reaction the surface composition was investigated by AES under UHV conditions. Figure 6 shows Auger spectra obtained after 30 min reaction at temperatures between 423 and 503 K, in comparison to the as-prepared catalyst (a 10 nm PdO layer obtained by oxidation at 673 K, as described above). The oxygen KLL signal at 505 eV declines after reaction at increasing temperature. Since AES is surface sensitive, this oxygen loss merely indicates a reduction of the PdO *surface*. In contrast, the total amount of oxygen, determined by thermal desorption, was nearly unchanged after all reactions. This means that during reaction mainly the surface layer is reduced and that oxygen loss from the bulk is small. The main signal of the spectra shown in figure 6 corresponds to the Pd $M_{4,5}VV$ transition. The peak from the as-prepared PdO sample is relatively small (lowest Pd content of the near-surface layers), but after reaction at increasing temperature it becomes more intense and changes its shape from symmetric to asymmetric. After reaction at 453 and 503 K it equals that arising from the clean Pd metal surface, but the corresponding oxygen signal still indicates a considerable amount of oxygen in surface-near layers. It is known that the line shape of the Pd $M_{4,5}VV$ auger transition resembles the shape of the valence band, since Pd is a band-like metal [19]. Pillo *et al.* [20] have observed similar changes of the XPS valence band spectra of PdO upon heating in UHV at 473 K. On the contrary, *ex-situ* Raman spectra obtained after reaction at 503 K showed no appreciable changes compared to the as-grown catalyst, again indicating that *bulk* structure and composition of PdO were not appreciably changed under reaction conditions.

4. Summary and conclusions

The reaction scheme of figure 7 may serve as a basis to rationalize the observed trends in selectivity and activity. It comprises the following reaction steps:

(1) Dissociation to C(ads), C(sub), H(ads) and H(sub)
(2) Reaction of C(ads) + O(ads) to CO and CO_2, of 2 H(ads) + O(ads) to water
(3) Reaction of C_2H_4(ads) with O(ads)
(4) Rearrangement of oxametallacycle to acetaldehyde
(5) Rearrangement of oxametallacycle to ethene oxide
(6) Oxidation of acetaldehyde to acetic acid
(7) Total oxidation of acetic acid

Starting from either Pd or PdO, the dissociation of ethene into carbon and hydrogen (via ethylidyne as intermediate [15,16]), followed by reaction to CO_2, is the predominant pathway, but the route to partially oxidized products (via molecularly adsorbed oxygen and π-bonded ethene [21] forming an oxametallacycle intermediate [14]) is more favoured on the PdO surface than

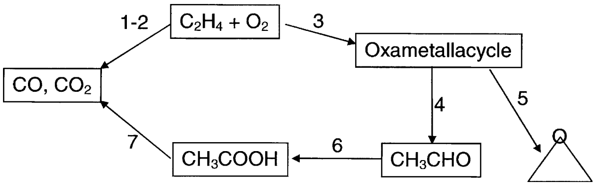

Figure 7. Reaction scheme for ethene oxidation on Pd containing catalysts. Reaction steps: (1) Dissociation of ethene, (2) Reaction of C(ads)+O(ads) to CO and CO_2, (3) Reaction of C_2H_4(ads) with O(ads), (4) Rearrangement to acetaldehyde, (5) Rearrangement to ethene oxide (6) Oxidation to acetic acid (7) Oxidation to CO_2.

on Pd metal, and the selectivity to acetic acid may reach 12% and more, depending on temperature, feed and reaction time.

On Pd metal, acetic acid is formed at lower temperatures than on PdO. Between 453 and 473 K its production is enhanced by modification of the surface with carbon. On stoichiometric PdO, activation for partial and total oxidation occurs during an induction period, leading to a partly metallic state of the surface phase after this initial reduction. Hence, under working conditions Pd metal, PdO, "PdC_x" and isolated defects are coexistent on the surface, and oxygen activation occurs either at defects or at the phase boundary between the oxidic, metallic and/or "PdC_x" phases. This surface is active for both CO_2 and acetic acid formation. The observed additional time delay with respect to acetic acid formation may be caused by a slow carbon uptake in the active phase.

The presence of an extended metal surface favours the follow-up oxidation of acetic acid above 473 K, but the presence of PdO stabilizes acetic acid at 493 K and beyond, On stoichiometric PdO acetic acid is stable up to 573 K in the presence of oxygen. Combining arguments we may conclude that highly dispersed metallic Pd centres on top of the PdO phase (or of any other support capable to stabilize selective oxidation products under reaction conditions) promote selective oxidation and suppress total oxidation of ethene.

Acknowledgments

We gratefully acknowledge research grants provided by the University of Innsbruck to W.U. and by the German Max Planck Society to H.G.

References

[1] P. Solomonsson, S. Johansson and B. Kasemo, Catal. Lett. 33 (1995) 1.
[2] D. Linke, D. Wolf, M. Baerns, O. Timpe, R. Schlögl, S. Zeyss and U. Dingerdissen, J. Catal. 205 (2002) 16.
[3] D. Linke, D. Wolf, M. Baerns, O. Timpe, S. Zeyss, U. Dingerdissen and L. Mleczko, Chem. Eng. Sci. 57 (2002) 39.
[4] J.A. Lopez-Sanchez, R. Tanner, P. Collier, R.P.K. Wells, C. Rhodes and G.J. Hutchings, Appl. Catal. A 226 (2002) 323.
[5] J.L. Seoane, P. Boutry and R. Montarnal, J. Catal. 63 (1980) 191.
[6] K. Sano, H. Uchida and S. Wakabayashi, Catal. Surv. Jpn. 3 (1999) 55.
[7] N. Mizuno, H. Ishige, Y. Seki, M. Misono, D.-J. Suh, W. Han and T. Kudo, Chem. Commun. (1997) 1295.
[8] C. Kemball and W.R. Patterson, Proc. Roy. Soc. Lond. A Mat. 270 (1962) 219.
[9] Y.-F. Han, D. Kumar and D.W. Goodman, J. Catal. 230 (2005) 353.
[10] H. Gabasch, W. Unterberger, B. Klötzer, K. Hayek, B. Aszalos-Kiss, D. Zemlyanov, E. Kleimenov, D. Teschner, Sp. Zafeiratos, M. Hävecker, A. Knop-Gericke, and R. Schlögl, in preparation.
[11] W. Reichl, G. Rosina, G. Rupprechter, C. Zimmermann and K. Hayek, Rev. Sci. Instrum. 71(3) (2000) 1495.
[12] K. Otto, C.P. Hubbard, W.H. Weber and G.W. Graham, Appl. Catal. B 1 (1992) 317.
[13] Landolt-Börnstein, Group IV Physical Chemistry, Volume 20 B, Springer-Verlag, Berlin, 2000.
[14] R.M. Lambert, R.M. Ormerod and W.T. Tysoe, Langmuir 10 (1994) 730.
[15] M. Bowker, C. Morgan and J. Couves, Surf. Sci. 555 (2004) 145.
[16] M. Bowker, C. Morgan, N. Perkins, R. Holroyd, F.E.F. Grillo and A. MacDowall, J. Phys. Chem. 109 (2005) 2377.
[17] J.R. McBride, K.C. Haas and W.H. Weber, Phys. Rev. B 44 (1991) 5016.
[18] A.C. Skapski and M.L. Smart, Chem. Commun. (1970) 658.
[19] M. Cini and C. Verdozzi, J. Phys.: Condens. Matter 1 (1989) 7457.
[20] Th. Pillo, R. Zimmermann, P. Steiner and S. Hüfner, J. Phys. Cond. Matter 9 (1997) 3987.
[21] G.A. Somorjai and K.R. McCrea, Adv. Catal. 45 (2000) 385.